Gould Jessica (Orcid ID: 0000-0001-6321-0409)

Linear extension and calcification rates in a cold-water, crustose coralline alga are modulated by temperature, light and salinity

Jessica Gould[1*], Justin B. Ries[1]

[1]Department of Marine and Environmental Sciences, Northeastern University, Nahant, MA, USA; ORCID ID 0000-0001-6321-0409; gould.je@northeastern.edu

[1]Department of Marine and Environmental Sciences, Northeastern University, Nahant, MA, USA; ORCID ID 0000-0001-8427-206X; j.ries@northeastern.edu

[*]**Correspondence**: Jessica Gould; j.gould@northeastern.edu

Keywords: coralline algae, calcification, growth experiment, temperature, light, salinity, linear extension

This is the author manuscript accepted for publication and has undergone full peer review but has not been through the copyediting, typesetting, pagination and proofreading process, which may lead to differences between this version and the Version of Record. Please cite this article as doi: 10.1002/lno.12474

Abstract

Long-lived crustose coralline algae are important ecosystem engineers and environmental archives in regions where observations of climate variability are sparse. *Clathromorphum compactum* is a cold-water alga that precipitates calcite that serve as archives of change at annual to sub-annual resolution. Understanding how environmental variability impacts the growth of this species is imperative for application in paleoclimate research, and for evaluating its vulnerability to change. Here, we present the results of the first, to-our-knowledge, controlled laboratory experiment isolating the effects of light, temperature, and salinity on calcification rates of *C. compactum*. Algal calcification rates were modulated by a combination of light exposure, salinity, and temperature, where temperature and salinity were positively correlated, and light level was negatively correlated with calcification rate. Linear extension of the skeleton also varied with treatment conditions, with the epithallial and perithallial layers of skeleton responding differently. Epithallial extension increased with salinity, while perithallial extension was governed only by a positive parabolic relationship with temperature. These results suggest that *C. compactum* growth will be impacted by environmental changes predicted for the Arctic over the coming decades. While increased temperature in the region may facilitate calcification in the algae, reductions in salinity associated with increased sea ice melt, and potentially increased light levels, may counteract this effect. The negative impact of increased light levels on algal calcification observed may not reflect the true impact of light availability on growth associated with a lengthening of the growing season (not evaluated in this study) accompanying reductions in annual sea-ice.

Introduction

The crustose coralline algal species *Clathromorphum compactum* is amongst the longest lived marine calcifiers in the world (Halfar et al., 2007; Adey et al., 2013), producing annual, high-magnesium calcite (mole-% $MgCO_3$ >15) layers that can be counted, dated, and chemically analyzed to reconstruct—at annual to sub-annual scale resolution—past environmental conditions in subarctic to arctic ecosystems, such as seawater temperature (e.g. Gamboa et al., 2010; Williams et al., 2014; Hetzinger et al., 2018;), seawater Mg/Ca (Ries, 2006), seawater pH (Anagnostou et al., 2019), primary productivity (Chan et al., 2017a), herbivory (Rasher et al., 2020), and sea ice cover (Halfar et al., 2013; Chan et al., 2017a; Hetzinger et al., 2019; Leclerc et al., 2021; 2022).

One of the reasons *C. compactum* serves as such a reliable marine archive, beyond its nearly cosmopolitan distribution, long lifespan, sessile nature, continuous growth, and annually layered skeleton (Halfar et al., 2008; Adey et al., 2013), is its relatively unique growth process. Growth of the algae initiates in the intercalary meristem, which is unique to this group of Rhodophyta, located between the outer photosynthetically active epithellial skeletal layers and the underlying bulk perithallial layers (Adey, 1964; Adey et al., 2005). Continuous accretion of calcite skeleton from the growth plane in *C. compactum* produces thick, mound-like, crusts upwards of ca. 50 cm, with growth occurring bilaterally from the meristem downwards into the perithallium and upwards into the epithallium. This mode of growth protects the archival skeleton (perithallium) from grazing and erosion by marine invertebrates, such as echinoids, limpets, and chitons (Adey, 1965; Steneck, 1982; Adey et al., 2013) and renders *C. compactum* perithallial skeleton a reliable paleoceanographic archive (Lebednik, 1976; Adey et al., 2015). Due to varying calcification rates over the annual cycle, driven by seasonal environmental

factors such as temperature and light availability, skeletal calcite accreted in winter months is less densely distributed than skeletal calcite accreted in summer months, resulting in intraannual cycles in skeletal density that can be visualized as annual banding with light microscopy, x-ray, or computed tomographic scanning ('CT scanning'), which can be used to age the alga (Adey et al., 2013; Chan et al., 2017b; Williams et al., 2021a).

In addition to serving as important climate archives, these algae play a key role in the marine ecosystem by providing a vast three-dimensional reef-like substrate and habitat for benthic organisms and larval settlement, serving as ecosystem engineers in some of the most fragile ecosystems on earth, and contributing to regional primary production and calcium carbonate deposition (Steneck, 1986; Chisholm, 2003; Adey et al., 2013; Chenelot et al., 2011, Rasher et al., 2020).

As *C. compactum* is primarily found between 10- and 20-meters depth along subarctic and arctic coastlines reaching from the northern coast of Maine to the Canadian Arctic (Adey et al., 2013; Adey, 1966), this species exhibits a tolerance for a wide range of naturally occurring thermal, light, and nutrient regimes (Adey et al., 2013). Growth rates examined in wild-collected *C. compactum* specimens vary substantially along the species' range, with growth in the southern more-temperate reaches of its distribution typically ranging from 300 to 500 μm $year^{-1}$, and growth in the northern, colder, and often sea-ice covered reaches of its distribution approaching ca. 100 μm $year^{-1}$ or less (Adey et al., 2013; Williams et al., 2021b). Likewise, growth of *C. compactum* slows in the cold, dark, winter months and increases in the warm, sunlit summer months (e.g., Adey et al., 2013; Williams et al., 2021b). Indeed, it is the reduced rate of skeletal extension under the lower light and temperature conditions of the winter months in the high-arctic that enables reliable reconstruction of interannual changes in temperature and sea ice

extent from the thickness of annual growth bands in *C. compactum* (e.g., Halfar et al., 2013; Leclerc et al., 2021).

Generally, crustose coralline algal growth is dependent on several physical and physiological factors, including seawater temperature, light availability, nutrient availability, salinity, and calcite saturation state (Adey, 1970; Halfar et al., 2011; Adey et al., 2013; Williams et al., 2018; 2021; Westfield et al., 2022). Much of the currently established understanding of *C. compactum* growth arose from extensive field-based observations and relatively sparse controlled laboratory experiments testing the effect of a subset of environmental factors, such as temperature, light, and pCO_2 on *C. compactum* growth and calcification (e.g., Williams et al., 2018; Westfield et al., 2022). The extent to which calcification in this species is driven by elevation of calcite saturation state at the site of calcification and other metabolic processes (Adey et al., 2013) is yet unresolved. However, it has been shown that certain species of crustose coralline algae substantially elevate pH and, thus, calcite saturation state, at the site of calcification (e.g., Anagnostou et al., 2019; Cornwall et al., 2017).

Although temperature appears to be a consistent and major determinant of growth rate in crustose coralline algal species (e.g., Adey et al., 1970; Halfar et al., 2011; Williams et al., 2018; Williams et al., 2021b; Westfield et al., 2022; Gould et al., 2022), the influence of other important environmental factors, such as light and salinity, are far less understood. For example, Westfield et al. (2022) investigated the isolated and interactive effects of increased temperature and pCO_2 on algal growth and calcification in *C. compactum* sampled from the Gulf of Maine and found normal parabolic responses to warming (i.e., highest growth at intermediate conditions), with varied response to increased pCO_2. Furthermore, while the effect of decreased salinity on *C. compactum* growth has yet to be explicitly and empirically studied, field

observations by Williams et al. (2021) from wild-collected specimens indicate that decreases in salinity (i.e., seawater freshening) may contribute to declines in growth rate in algae from the northwest Atlantic and Canadian Arctic. Furthermore, controlled laboratory experiments show that *Leptophytum foecundum* exhibits a stress response to low salinity (Muth et al., 2020).

Environment changes in the Arctic Ocean are occurring at a rate nearly twice that of the global average in response to anthropogenic disturbance (Kaufman et al., 2009; Kinnard et al., 2011; Spielhagen et al., 2011; Rodrigues, 2009). Among the many rapidly changing parameters in this region, we know little about the long-term dynamics of sea-ice, salinity, and under-sea-ice ocean temperatures. Precipitous changes in the Northwest Atlantic and Arctic Oceans, such as rising seawater temperature, seawater freshening associated with the increased melting of sea ice, glaciers, and ice sheets, and changing seafloor light-regimes, will likely impact not only the growth rate of *C. compactum*, but also their resistance to herbivory (i.e., grazing through the epithallial skeleton, penetrating beyond the meristem and impeding growth) and physical erosion (e.g., wave action, ice scouring) (Rasher et al., 2020; Williams et al., 2021(a); Westfield et al., 2022). Loss of algal mass to the ecosystem will likely cause important shifts in ecosystem dynamics, as well as a reduction in oceanic primary productivity and calcium carbonate production. Therefore, a more complete understanding of temperature, salinity and light level control on *C. compactum* growth and survival is necessary both for paleoenvironmental applications and for understanding the fate of this species in the face of climate change.

Here, we present the results from a three-month controlled laboratory experiment isolating the effects of light level, temperature, and salinity on the rates of net calcification and extension (vertical growth) of *C. compactum* specimens collected from Arctic Bay, Nunavut, Canada. The experiment tests the specific hypotheses that (1) algal growth increases with

increased seawater temperature, (2) algal growth decreases with decreased salinity and (3) growth increases with increased light availability. To our knowledge, this works yields the first empirical constraints on the isolated effects of salinity on the skeletal extension and calcification of this species. The results presented have implications for both the fate of *C. compactum* in a changing Arctic, and for improved understanding of paleoceanographic records obtained from these algae.

Methods

Sample preparation and experimental setup

Specimens of *Clathromorphum compactum* used in this study were collected in March 2020 from 15 meters depth in Arctic Bay, Nunavut, Canada (73º 01' 011''N, 85º 09' 155''W) (Figure 1). The high latitude location of the chosen study site for this laboratory manipulation experiment allows for the evaluation of growth rates in algal specimens from a latitude that is often sampled from for reconstruction of historical sea-ice extent and temperature in the High Arctic. Algae were sampled by SCUBA and transported live to Northeastern University's Marine Science Center in thermoregulated containers wrapped in cloth wetted with seawater to keep from drying out in transit. Upon arrival, algae were held in flow-through tanks supplied with seawater from Broad Sound, Massachusetts Bay (salinity 31), chilled to a temperature of 3ºC, and exposed to 12-hour intervals of alternating light (ca. 25 µmol photons m^{-2} s^{-1}) and dark throughout the experiment, including during a three-week acclimation prior before the start of the experiment.

A total of 40 *C. compactum* colonies were collected from Arctic Bay, NU, and sectioned into smaller ca. 1-3 cm^2 segments using an Inland Craft™ SwapTop lapidary saw equipped with a 6'' diamond-embedded saw blade, yielding five to six algal fragments for each of the 36

experimental tanks. All algal fragments were assigned unique identification numbers to track individual and colony and affixed to a plastic microscope slide with nontoxic cyanoacrylate adhesive and anchored with a glass bead. The potential for a colony-level effect was controlled for by including algal colony as a random effect in statistical modeling.

After the three-week laboratory acclimation period, all algal fragments were submerged in seawater mixed with calcein dye (3 mL 1% calcein solution/L-seawater; Western Chemical *SE-MARK*). This non-toxic fluorescent dye is incorporated into the growing algal skeleton over the course of 72 hours and allows for identification of algal skeleton formed exclusively during the experiment. Flow-through seawater to the holding tanks was shut off during the 72-hr calcein-staining period to maintain the calcein at the required concentration within the tanks, after which the tanks were flushed with fresh seawater. Calcein staining tanks were held at the temperature conditions previously maintained throughout the acclimation. After calcein staining, algae were randomly assigned to a treatment tanks maintained at the target light level. Seawater temperatures were either ramped up or down over the course of two days from the 3 ºC acclimation temperature to the treatment condition and desired salinity treatment levels were reached across these two days by increasing flow of desired seawater to each tank with controlled flow-meters at a rate of 60 mL min^{-1}. A short period of two-days was used to adjust tanks to treatment levels due to restrictions to access of the experimental array set by COVID guidelines in March of 2020, and should be considered when interpreting the results. The upper surface of the algae were lightly scrubbed with a nylon brush throughout the experiment to remove any accumulation of particulate matter and to roughly mimic the grazing of their epithallial layer that occurs in the wild. Of the 200 algal fragments used in this experiment, 21 were removed from the experiment on day 56 due to severe loss of pigmentation. An additional

28 algal fragments were removed from analysis due to detachment from the plastic slide during buoyant weighing, rendering buoyant weights inaccurate. A total of 49 algal fragments are therefore not included in the results presented here, yielding a total algal sample size of 151.

The experimental design consisted of a total of 36 42-L acrylic tanks, each formulated with a unique combination of temperature (2.5, 4, 5.5, 7, 8.5, 10 °C), light [low (20 µmol photons m^{-2} s^{-1}), medium (120 µmol photons m^{-2} s^{-1}), high (250 µmol photons m^{-2} s^{-1})], and salinity (28, 31) (refer to Figure S1 for experimental design). The ranges in salinity and temperature chosen are reflective of current conditions expected in the region and potential future warming and freshening (lower salinity) scenarios in the Arctic region. The light treatment levels were modeled after the Westfield et al. 2022 laboratory experiment on *C. compactum* collected from the Gulf of Maine. Each shelf in the experimental array consisted of three treatment tanks connected to a dedicated 95 L sump outfitted with both a physical mesh filter and activated carbon filter and an *Eshopps PSK-75* protein skimmer. The potential for a sump-level effect was controlled for by including sump tank as a random effect in statistical modeling. Natural seawater treated with ultraviolet radiation and filtered with 5 µm filters was supplied at an average rate of 60 mL min^{-1} to the 31 salinity treatment tanks throughout the experiment. The same seawater was first mixed with reverse osmosis deionized water to achieve the 28 salinity treatments before feeding into the low salinity tanks at an average rate of 60 mL min^{-1} throughout. Compressed ambient air was continuously bubbled into the tanks throughout the experiment using flexible air bubblers controlled by *Darhor* needle-valve flow controllers at approximately 1 L min^{-1}, which ensured that the seawater was in equilibrium with the water with respect to pCO_2. Each treatment tank was covered with an acrylic lid to trap the bubbled air in

the headspace of the tank to facilitate gas-water equilibration and minimize evaporative water loss.

Temperatures were maintained with *Coralife* ¼ HP aquarium chillers, with a capacity to chill to a minimum of 2.5 °C in this system. Light levels consisted of three treatments set to 12 h dark and light periods: low (20 µmol photons m^{-2} s^{-1}); medium (120 µmol photons m^{-2} s^{-1}); and high (250 µmol photons m^{-2} s^{-1}) at the height of the algae, which were mounted on an elevated platform to maintain access to light and sufficient water flow around the specimens. One or two *Ecoxotic Panorama Pro* 16W 12,000K/445nm white/blue LED modules (depending on light treatment) were installed 10 cm above each platform and set to the intensity required to achieve the target light levels. Light levels were measured using an *Apogee MQ-200X Quantum Sensor* and handheld meter.

Experimental seawater monitoring

Temperatures and salinities of the seawater in the treatment tanks were measured every three days throughout the 96-day experiment (Table 1). Temperature measurements were made with a NIST-calibrated glass thermometer (precision ±0.3%; accuracy ±0.4%), and salinity was measured with a YSI3200 conductivity electrode calibrated with Dickson standard seawater certified reference material.

Quantification of algal growth

Calcification rate

Net algal calcification rates were quantified using an empirically calibrated buoyant weight methodology (see Ries et al., 2009, for details). In brief, algae were buoyantly weighed in seawater set at a constant temperature of 6 °C and salinity of 29, using a bottom loading balance (*Nimbus NBL 423e Precision Balance*, precision = 0.0002 g, accuracy = 0.002 g) at the start of

the experiment (i.e., immediately after calcein staining), after 39 days of exposure, after 71 days of exposure, and at the conclusion of the experiment (96 days). After the final buoyant weight measurement, algae were air dried for 14 days, after which each fragment was removed from the plastic slide and dry-weighed with a bench-top balance (*Nimbus NBL 423e Precision Balance*, precision = 0.0002 g, accuracy = 0.002 g). All buoyant weights were converted to empirically derived dry weights for quantification of net calcification using the linear relationship between the end-of-experiment dry weights and corresponding buoyant weights (Dry Weight (g) = 1.66±0.01(Buoyant Weight (g)) – 0.58±0.01, $p < 2.2\text{x}10^{-16}$, $R^2 = 0.99$, $SE = 0.05$, $n = 151$, Figure 2). Net calcification rate (mg cm^{-2} day^{-1}) was then calculated as the change in dry weight of the algal fragment per day across the interval that the alga grew under experimental conditions, normalized to the upper surface area of the algal fragment. Algal fragment surface areas were quantified from photographs taken at the beginning of the experiment with the imaging software *ImageJ*.

Linear extension

At the conclusion of the experiment, all algal fragments were sectioned to a thickness of 4 to 5 mm with an *Isomet* petrographic trim saw using a diamond-embedded blade at slow speed lubricated with tap water. Sections were ground flat using an *Accutom* precision grinder, sequentially polished with polishing grits ranging from 90µm to 3µm and mounted to glass slides with *Crystalbond* epoxy. Linear extension of the algal fragments during the experiment was quantified by first locating the calcein layer that marks the initiation of the experiment using a Nikon AZ100 diascopic microscope equipped with a D90 digital SLR camera and a blue, fluorescent light filter block (440 to 460 nm; Figure S3). Linear extension was measured as the vertical distance in microns from the calcein line upwards to the meristem for the perithallial

measurement, and from the meristem upwards to the algal surface for the epithallial measurement. Average linear (vertical) extension rates (μm day^{-1}) were quantified by dividing the total area of skeletal cross section (μm^2) above the calcein marker (perithallial measurement) or meristem (epithallial measurement) by the total length of the calcein marker or meristem (μm), normalized to algal growing days.

Whenever possible, linear extension was quantified separately for the epithallial skeletal layer and perithallial skeletal layer, and for both layers in aggregate (Figure S3). Importantly, it was not possible to constrain the thickness of epithallial layer that was formed prior to the experiment (i.e., in the wild), and unfortunately the calcein stain was not recorded in the epithallial skeletal layer in this experiment. Instead, the measurements of epithallial vertical extension are made from the meristem to the surface of the algae, which inherently includes epithallial skeleton accreted prior to the experimental period. However, it is expected that the initial epithallial skeletal layer thickness would have varied randomly across all algal colonies, and because each algal fragment was randomly distributed in the experimental design, and any difference in initial epithallial skeletal layer thickness should be normally distributed in final epithallial thickness measurements and thus not bias the trends observed in the study.

Skeletal density

Total algal skeletal densities (mg cm^{-3}, Eq. 1) were derived by dividing net calcification (mg cm^{-2}) by linear extension (cm). Because linear extension measurements on the algal fragments in this study were measured across only one representative cross-section of the alga's growing surface, this approach to quantifying algal skeletal density assumes that mean extension across this section was representative of mean extension across the entire surface of the algal skeleton. To parameterize algal skeletal density values obtained in this manner within a positive

domain, the algal density dataset was restricted to include only algal fragments that exhibited net positive calcification rates over the course of the experiment. Also eliminated were outliers with empirically derived density estimates above 2,710 mg cm^{-3} (the density of pure calcite without any porosity) and below 700 mg cm^{-3} (lowest density of *Clathromorphum* skeleton observed in Williams et al., 2021).

$$\text{Total Density}\left(\frac{\text{mg}}{\text{cm}^3}\right) = \frac{\text{total calcification } (\frac{\text{mg}}{\text{cm}^2})}{\text{Total}_{\text{LE}}\ (\text{cm})} \qquad \text{(Eq 1)}$$

Statistical analysis

Random intercept linear mixed effects models (LMER) were used to test the fixed effects of temperature, light, and salinity on the response variables of skeletal linear extension, total calcification rate, and total density. Temperature, salinity, and light are treated as continuous fixed effects in all models. Colony and sump were included as random effects to account for colony- or sump-level effects on the measured outcomes. Final model selection was performed using the step() function in the R package lmerTest, which conducts backward model reduction by first eliminating random effects (eliminated if $p > 0.1$), and then fixed effects (eliminated if $p > 0.05$), from each model using Likelihood Ratio Testing. In all cases, the random effect of colony and sump were not significant. As random effects were not included in any model, linear regression analyses using the base R function lm() was used to define individual relationships between the response variables of interest and treatment conditions, using AIC scores to select between linear, second-, third- and fourth-order polynomials. R^2 values for the final model selections are reported as marginal R^2 values. All model assumptions were evaluated using diagnostic residual-fitted value plots and Q-Q plots, and, if required, response variables were

log-transformed to conform to the assumption of normality. All statistical analyses were conducted using the open-source R statistical software (version 1.4.1717, RStudio, PBC).

Results

Calcification rate

Most algal fragments (129 of 151) exhibited positive net calcification rates, with 22 algae exhibiting net dissolution (i.e., negative net calcification rates) although determination of gross dissolution rates could not be determined from the data at hand. A total of seven outliers falling outside the interquartile range were identified and removed from further analysis, resulting in a total sample size to 144 algal fragments. Overall, calcification rates ranged from -0.16 mg cm^{-2} day^{-1} to 0.58 mg cm^{-2} day^{-1}, with an average (*SE*) of 0.17 (0.01) mg cm^{-2} day^{-1} (N = 144, Table 2) across all treatments. Evaluated independently, calcification rates increased significantly with increased seawater temperature and salinity; however, calcification rates declined with increased light level (Figure 3). Temperature had the strongest effect on total algal calcification rate (Figure 3; p-value <0.0001). Salinity and light had smaller and opposite effects on total algal calcification rate, where every unit increase in salinity increases average calcification rate by 0.024 mg cm^{-2} day^{-1}, and every unit increase in light level decreases average calcification rate by 0.0004 mg cm^{-2} day^{-1} (Figure 3).

A LMER model evaluating calcification rate as a function of the additive and interactive effects of temperature, salinity, and light indicates that calcification rate was best modeled as a function of the additive effects of temperature (non-linear), salinity, and light (Table 3), where neither the random effects of sump nor colony were significant predictors of algal calcification rate. Interestingly, calcification rate increased similarly with temperature for algal specimens growing in the higher salinity treatment (31 target salinity) across all levels of light exposure as

compared with algal specimens growing in low-salinity (28 target salinity) treatment at mid- and high-light levels (Figure 4). While the interactive effect of light and salinity was not a significant predictor of calcification rate in the model, Figure 4 indicates suggests that low-salinity conditions combined with mid- or high-light levels had additive negative effects on algal calcification rates.

Linear extension

A total of 90 of the 144 algae included in the calcification rate analyses exhibited strong and clearly identifiable perithallial calcein horizons, with total, epithallium, and perithallium extension differentiable within 85 of these. Total linear extension rate, defined as the average thickness of skeletal extension from the onset of the experiment (the calcein marker) to the outer surface of the algae (including the epithallium) is positively, linearly correlated with algal calcification rate (Figure S2, $p = <0.01$). The observation that many of the 22 algal fragments exhibiting negative calcification rates accreted new skeleton, as observed by measurement of vertical extension relative to the calcein marker, indicates that algae losing overall mass were still extended the perithallial skeleton throughout the experiment.

Overall, across all treatments, the algal fragment thallus (perithallium and epithallium) extended between a minimum of 0.44 μm day^{-1} and a maximum 3.37 μm day^{-1}, with an average (*SE*) total linear extension rate of 1.53 (0.06) μm day^{-1}. LMER analysis evaluating total linear extension as a function of the additive and interactive effects of temperature, salinity, and light indicates that total linear extension rate was best modeled solely as a function of temperature (Table 3). Average total linear extension rate increased linearly with temperature ($\alpha = 0.05$, $p < 0.05$), with average extension rate increasing by 0.05 μm day^{-1} for every unit increase in temperature (Figure 5; Table 3).

Log-transformed epithallium linear extension rate was positively correlated with salinity ($\alpha = 0.05$, $p < 0.001$, Table 3) and weakly negatively correlated with light (statistically significant at the 90% confidence level ($\alpha = 0.10$, $p = 0.07$) (Figure 5). Finally, a positive-threshold relationship was observed between perithallium linear extension rate and temperature in the best-fit model identified by lowest AIC score ($\alpha = 0.05$, $p < 0.01$, Table 3 and Figure 5). On average, perithallial linear extension occurred at approximately twice the rate of epithallial linear extension [mean (*SE*) perithallial linear extension rate = 1.08 (0.06) μm day^{-1}, mean (*SE*) epithallial linear extension rate = 0.47 (0.02) μm day^{-1}], which is expected given the smaller cell size of the epithallial skeletal layer.

Skeletal density

Total skeletal density (mg cm^{-3}) of the new skeleton formed during the experiment was derived by dividing net calcification (mg cm^{-2}) by total linear extension (cm). After eliminating samples that exhibited skeletal densities outside of a reasonable range (see methods), total skeletal density values ranged from 701.8 to 2650.4 mg cm^{-3}, with an average (*SE*) of 1667.8 (82.2) mg cm^{-3} ($n = 52$). Mean density of the newly formed skeleton was not significantly correlated with treatment.

Discussion

The impact of temperature, light, and salinity on algal calcification rate relative to current knowledge

We found that total algal calcification rate in these *C. compactum* specimen (i.e., perithallial plus epithallial layers) varied as a function of temperature, salinity, and light level, with temperature exhibiting the strongest control (Figure 3, Table 3). Calcification rates were best modeled as a polynomial function of temperature, increasing at the low (2.5-5°C) and high (8.5-11°C) end of the temperature treatments, and plateauing between 6 and 8.5°C. The non-

linear nature of this relationship is in part driven by reductions in calcification for algal specimens growing in low-salinity and mid-to-high-light treatments (Figure 4). When parsed across salinity and light treatment conditions, most calcification in the algal specimen examined here showed a linear increase with increasing temperatures (Figure 4). The overall finding that calcification rates increase with temperature is in alignment with previous observations of wild specimens, where calcification rates in algae growing in lower-latitude, warm water regions are generally faster than for algae collected from colder, higher latitude waters (e.g., Williams et al., 2021b). Indeed, Williams et al. (2021b) indicate that temperature rather than light availability was likely the driving factor of increased calcification rate for a collection of wild specimens sampled across a north-south range. In addition to observations in wild specimens, Williams et al. (2018) and Westfield et al. (2022) show that growth rate and calcification rate in *C. compactum* increases with increased growth temperature in controlled laboratory experiments.

Increased light exposure across treatments in the present study resulted in decreased calcification rates. The overall negative impact of increased light on calcification rates observed does not align with previous work showing that increased irradiance increases rates of growth and calcification in coralline algae. For example, Bélanger and Gagnon (2021) observed increased growth rate with increased irradiance for the subarctic rhodolith-forming crustose coralline alga *Lithothamnion glaciale*. The reduction in calcification at high light observed in the present study (Figure 3) may instead be explained by the likelihood that these high-arctic specimens are adapted to low-light conditions, potentially causing the elevated light conditions in the present experiment to induce a stress response. Although measurements of photosynthetic activity were beyond the scope of this experiment, it is conceivable that photoinhibition occurred above light levels of 160 µmol photons m^{-2} s^{-1}, as observed in Roberts et al. (2002). Furthermore,

exposure to mid- and high-light levels in this experiment appear to have been the most deleterious for algae growing in the low salinity treatment, and that while not statistically significant at the 95% confidence level, an interactive effect of light and salinity may be exacerbating the observed reduction in algal calcification rate with increasing light (Figure 4).

Finally, we show here for the first time in a controlled experiment, that skeletal calcification in *C. compactum* decreases with decreasing salinity (Figure 3; Figure 4). This finding is consistent with Muth et al. (2020), who demonstrate a similar impact of low salinity on calcification within *Leptophytum foecundum*. Williams et al. (2021) also deduced the existence of this relationship for wild *C. compactum* based on an apparent decline in net calcification rates along a latitudinal gradient in the northeast Atlantic and Arctic Oceans.

Impact of temperature, light, and salinity on skeletal linear extension relative to current knowledge

Linear extension of the total algal skeleton across the experimental period is best modeled as a linear function of temperature, where total skeletal extension increases with temperature. Variable responses of skeletal extension to temperature have been previously described in both algal culture work (Steller et al., 2007; Kamenos & Law, 2010; Williams et al., 2018; Cornwall et al., 2019 and references therein) and investigations of wild specimens across latitudinal temperature gradients (e.g., Adey et al., 2013, Williams et al., 2021b). Studies describing the linear extension of the *C. compactum* skeleton have typically focused on the perithallial skeleton, as this layer represents the bulk of the algal skeleton, remains relatively undisturbed from biological and physical erosional processes, and is more often used in paleoenvironmental reconstruction. The present study expands evaluation of algal skeletal extension to include both the perithallial and epithallial layers.

Interestingly, we find that the linear extension of the epithallial skeletal layer, which is the photosynthetically active layer of the *C. compactum* alga, is impacted most strongly by salinity, with linear extension increasing with salinity. Here, by empirically isolating the effect of salinity on algal extension rate, we find that extension of only the epithallial skeleton, and not the perithallial skeleton, is negatively impacted by decreasing salinity. Because there was no significant relationship between algal total density and the treatment conditions, we posit that the observed decline in calcification rates with decreasing salinity is a result of this decline in extension of the epithallial skeletal layer. We hypothesize that salinity may not have significantly impacted the linear extension of perithallial skeleton due to the physical isolation of the perithallial skeletal crystal growth environment from the external seawater by the meristem and epithallial tissue layers above it. The exact mechanism behind the reduced calcification rates at lower salinity remains unclear. However, it may be a result of the reduced calcium ion concentration of the seawater ($[Ca^{2+}]$), as recent experimental work shows that low salinity combined with low $[Ca^{2+}]$ interactively reduce calcification rates of mussels from the Baltic Sea (Sanders et al., 2021).

We also identify a relationship between epithallial skeletal extension and light level in the experiment ($p = 0.07$), with epithallial skeleton extending less at higher light levels. Because this skeletal layer is the photosynthetically active layer, we initially hypothesized that increased light availability would improve the efficiency and output of photosynthesis and, therefore, skeletal extension. A previous experimental study by Williams et al. (2018) found that increasing irradiance increased overall growth of *C. compactum* across an 11-month experimental interval. In addition, much of the previously published work on wild specimens of *C. compactum* observed increased extension in algae growing at lower latitudes, where algae experience both a

longer growing season than arctic algae as well as increased irradiance at depth (e.g., Williams et al., 2021b). However, Adey et al. (2013) showed that *Clathromorphum* growth is most strongly driven by temperature and that light availability impacts skeletal density more than skeletal extension. We find here that increased light level caused a reduction in epithallial linear extension. Rather than stimulating photosynthesis, we posit that the elevated levels in the present experiment initiated photoinhibition within the algal epithallial skeletal layer. This assertion is supported by the fact that the lower perithallial skeletal layer, which is physically shaded from direct light, did not exhibit this inverse correlation between light and extension rate (see Figure 5, Table 3). Although a more detailed exploration of algal photosynthetic activity is beyond the scope of the present work, a qualitative evaluation of algal coloration at the conclusion of the experiment identifies a reduction in algal pigmentation in response to higher light levels, consistent with the assertion that the inverse correlation between light level and extension rate for the epithallial layer is driven by photoinhibition (Supplement Figure S4). Since skeletal density of the epithallial layer did not appear to change in this experiment, we deduce that the reduction in total algal calcification rates under elevated light is a consequence of the observed reduction in linear extension of the epithallial layer.

Finally, we find that linear extension of the perithallial skeleton is best modeled as a function of temperature alone. Extension rates in this layer were highest at warm experimental treatments and are best modeled as a nonlinear, punctuated positive relationship, where calcification rates increase with temperature in a step-wise fashion. This relationship is biologically realistic, as we expect the coralline algae sampled from the Arctic to increase extension with temperature towards the species' local thermal optimum of around 10 °C (Adey & Steneck, 2001; Adey et al., 2013). In addition, it has been shown that abiotic calcite

precipitation is strongly controlled by temperature (e.g., Burton et al., 1987), where precipitation occurs more rapidly under warmer seawater temperatures. The non-linearity of the algal growth response to temperature also aligns with findings of Halfar et al. (2011), in which perithallial growth layers of *C. compactum* were only strongly correlated with seawater temperature records in the cold North Atlantic region (i.e., the steeper, lower part of the curve in Figure 8). However, the relationship weakens in warmer regions of the Bering Sea, suggesting stronger control of calcification by temperature in the lower-temperature range for this species–consistent with results of the present study.

The fate of *C. compactum* in a changing Arctic Ocean

Changes to the Arctic Ocean expected over the coming decades have the potential to impact the growth and survival of *C. compactum*. How the combined effects of this environmental variability (e.g., increased seawater temperature, decreased salinity, increased pCO_2) will ultimately shape subarctic and arctic communities of crustose coralline algae are difficult to predict. The present study provides a lens through which we can evaluate the *C. compactum* growth response to three of these environmental factors that are predicted to change over the coming decades: temperature, salinity, and light availability.

While our results show that total algal calcification and linear extension rates of *C. compactum* are likely to increase with warming that is predicted for the near future (Figure 3), we also show that expected declines in Arctic Ocean salinity associated with warming waters will have a negative impact on algal calcification. Specifically, the linear extension of the sacrificial, photosynthetically active epithelial layer in our experiment was negatively impacted by declining salinity and increasing light level. In contrast, the extension of the perithallial

skeletal layer below the meristem, which comprises the bulk of the algal skeleton, increased with temperature.

We conclude that increases in seawater temperature and decrease in salinity expected to occur in some regions of the Arctic and in many regions of the Subarctic are likely to impact both the extent of crustose coralline algae in the benthic environment, as well as this species' ability to mineralize their calcitic skeletons, with potentially far-reaching impacts on the physical integrity of rhodolith-maerl deposits and the ecosystems that they support. Regardless of mechanism, a potential implication of low salinity may be a reduction in the thickness of the protective epithallial skeletal layer. Because the epithallial skeleton protects both the meristem tissue and perithallial skeleton, any reduction in the growth of this layer may impact the alga's ability to withstand grazing pressure (Rasher et al., 2020).

Finally, the decline in sea-ice extent in the Arctic Ocean that is expected over the coming decades is likely to increase both the duration of the growing season (due to reduction in duration and extent of sea-ice) and the intensity of light availability on the seafloor (due to thinning of sea-ice) where *C. compactum* is found. Conceivably, a longer growing season with increased temperature and light availability could increase algal growth rate (Bélanger & Gagnon 2021; this study), but the extent to which increased irradiance will remain beneficial for *C. compactum* is unknown. Our experiment reveals the deleterious effects of high irradiance on rates of calcification and linear extension, and the potential for photoinhibition in this species. However, hard conclusions regarding the impact of longer growing seasons on the growth of *C. compactum* cannot be drawn from the results of this experiment.

Implications for paleoenvironmental reconstructions

The relationship between sea-ice thickness and algal growth is used to reconstruct historical variations in sea-ice cover (Halfar et al., 2013; Hetzinger et al., 2019; Leclerc et al., 2021). Therefore, any environmental control on algal growth that is either decoupled from sea-ice cover and/or has a confounding (i.e., interfering) effect on extension will introduce error and uncertainty into this proxy. Here, we find that increased temperature is reflected in both an increase in total algal calcification rate and in perithallial linear extension—the skeletal layer used in paleoenvironmental reconstructions. However, light exposure did not impact perithallial linear extension (only epithallial linear extension) across the treatment conditions, a seemingly necessary relationship underpinning the algal growth banding proxy for sea-ice cover If an increase in growing season due to a lack of sea-ice cover causes thicker annual banding, one would expect increased light exposure to stimulate skeletal extension in the controlled experiments—which was not observed across all algal specimens in the present experiment. However, when the algae exposed to the low-light treatment in the experiment are evaluated separately from algae exposed to the mid- and high-light level treatments, there is indeed a positive linear relationship between perithallial linear extension rate and light level under the lower light conditions (3 to 23 μmol photons m^{-2} s^{-1}; Figure S5). If these lower light conditions are more reflective of the low-light environment in the Arctic Ocean at 15 m depth, this finding is consistent with Halfar et al.'s (2013) observation that algal growth band thickness increases with the duration of ice-free periods. Although promising, this result should be caveated by the fact that only light level, and not duration of light, was varied in our experiment - which does not fully reflect the natural variation in light associated with the annual waxing and waning of sea-ice. Importantly, because low salinity in our study only impacted linear extension in the outer

epithallial layer and not the perithallial layer that produces the layered portion of the skeleton used in paleoenvironmental reconstructions, these findings suggest that growth band thickness of *C. compactum* is not a viable proxy for seawater salinity. Likewise, we conclude that there may be no need to account for the effects of salinity when reconstructing extent of sea-ice cover from annual perithallial growth band thickness of *C. compactum*. However, future experiments examining the effect of salinity across a greater number of salinity treatments may prove insightful.

Conclusion

Linear extension and calcification rates of both the perithallial and sacrificial epithallial skeletal layers of *C. compactum* are impacted differently by temperature, salinity, and light. The perithallial layer exhibits rates of linear extension and calcification that increase with temperature. The epithallial skeletal layer exhibits reduced rates of calcification and linear extension under decreased salinity and increased light, the latter potentially due to photoinhibition of the algae. These responses portend future challenges for this species arising from decreasing salinity and increasing light levels that may result from future warming and the associated melting of glaciers and sea-ice, especially if impairment of the sacrificial epithallial layer allows grazers to more easily damage the meristem tissue that produces both skeletal layers. Future studies on this topic should evaluate the effects of duration of light exposure on algal calcification rate to explore the effects of future changes in the seasonal duration of sea-ice, evaluate effects of salinity, temperature, and light on algal photosynthetic rate and biomineral ultrastructure, and investigate the mechanism (e.g., $[Ca^{2+}]$) behind the observed decline in rates of calcification and skeletal extension with reduced salinity.

Literature Cited

Adey, W.H. (1964) The genus *Phymatolithon* in the Gulf of Maine. *Hydrobiologia,* 24, 377-420. doi: 10.1007/BF00170412

Adey, W.H. (1965) The genus *Clathromorphum* (Corallinaceae) in the Gulf of Maine. *Hydrobiologia,* 26(3), 539-573. doi: 10.1007/BF00045545

Adey, W.H. (1966) The distribution of *Saxicolous* crustose corallines in the northwestern North Atlantic. *J Phycol*, 2, 49-54. doi: 10.1111/j.1529-8817.1966.tb04593.x.

Adey, W.H. (1970) The effects of light and temperature on growth rates in boreal-subarctic crustose corallines. *J Phycol,* 6, 269-276. doi: 10.1111/j.1529-8817.1970.tb02392.x

Adey, W.H. & Steneck, R. (2001) Thermogeography over time creates biogeographic regions: A temperature/space/time-integrated model and an abundance-weighted test for benthic marine algae. *J Phycol*, 37, 677-698. doi: 10.1046/j.1529-8817.2001.00176.x

Adey, W.H., Chamberlain, Y., & Irvine, L. (2005) An SEM-based analysis of the morphology, anatomy, and reproduction of *Lithothamnion tophiforme* (Esper) unger (Corallinales, Rhodophyta), with a comparative study of associated North Atlantic Arctic/Subarctic Melobesioideae. *J Phycol*, 41, 1010-1024. doi: 10.1111/j.1529-8817.2005.00123.x

Adey, W.H., Halfar, J., & Williams, B. (2013) The coralline genus *Clathromorphum Foslie* emend. Adey: biological, physiological, and ecological factors controlling carbonate production in an arctic-subarctic climate archive. Smithsonian Contributions to the Marine Sciences (Smithsonian Institution Scholarly Press, Washington, DC), Vol 40, pp 1-48.

Adey, W.H., Halfar, J., Humphreys, A., Suskiewicz, T., Belanger, D., Gagnon, P., et al. (2015) Subarctic rhodolith beds promote longevity of crustose coralline algal buildups and their climate archiving potential. *Palaios,* 30(4), 281-293. doi: 10.2110/palo.2014.075

Anagnostou, E., Williams, B., Westfield, I., Foster, G.L., Ries, J.B., 2019, Calibration of the pH-δ11B and temperature-Mg/Li proxies in the long-lived high-latitude crustose coralline red alga *Clathromorphum compactum* via controlled laboratory experiments, *Geochim Cosmochim Ac*, 254, 142-155. doi: 10.1016/j.gca.2019.03.015

Bélanger, S., Babin, M., & Tremblay, J.É. (2013) Increasing cloudiness in Arctic damps the increase in phytoplankton primary production due to sea ice receding. *Biogeosciences*, 10, 4087-4101. doi: 10.5194/bg-10-4087-2013

Bélanger, D. & Gagnon, P. (2021) High growth resilience of Subarctic rhodoliths (*Lithothamnion glaciale*) to ocean warming and chronic low irradiance. *Mar Ecol-Prog Ser*, 663, 77-97. doi: 10.3354/meps13647

Burton, E.A. & Walter, L.M. (1987) Relative precipitation rates of aragonite and Mg calcite from seawater: Temperature or carbonate ion control? *Geology,* 15(2), 111-114. doi: 10.1130/0091-7613(1987)15<111:RPROAA>2.0CO;2

Chan, P., Halfar, J., Adey, W., Hetzinger, S., Zack, T., Moore, G.W.K., et al. (2017a) Multicentennial record of Labrador Sea primary productivity and sea-ice variability archived in coralline algal barium. *Nat Commun*, 8. doi: 10.1038/ncomms15543

Chan, P., Halfar, J., Norley, C.J.D., Pollmann, S.I., Adey, W., & Holdsworth, D.W. (2017b) Micro-computed tomography: Applications for high-resolution skeletal density determinations: An example using annually banded crustose coralline algae. *Geochem Geophy Geosy*, 18(9), 3542-3553. doi: 10.1002/2017GC006966

Chenelot, H., Jewett, S.C., & Hoberg, M. K. (2011) Macrobenthos of the nearshore Aleutian Archipelago, with emphasis on invertebrates associated with *Clathromorphum Nereostratum*

(Rhodophyta, Corallinaceae). *Mar Biodivers*, 41(3), 413-424. doi: 10.1007/s12526-010-0071-y

Chisholm, J.R.M. (2003) Primary productivity of reef-building crustose coralline algae. *Limnol Oceanogr, 48,* 1376-1387. doi: 10.4319/lo.2003.48.4.1376

Cornwall, C., Comeau, S., & McCulloch, M. (2017). Coralline algae elevate pH at the site of calcification under ocean acidification. *Glob Change Biol,* 23, 4245-4256. doi: 10.1111/gcb.13673

Cornwall, C.E., Diaz-Pulido, G. & Comeau, S. (2019) Impacts of ocean warming on coralline algal calcification: Meta-analysis, knowledge gaps, and key recommendations for future research. *Front Mar Sci*, 6. doi: 10.3389/fmars.2019.00186

Frantz, B.R., Foster, M.R., & Riosmena-Rodriguez, R. (2005) *Clathromorphum nereostratum* (Corallinales, Rhodophyta): The oldest alga? *J Phycol*, 41(4), 770-773. doi: 10.1111/j.1529-8817.2005.00107.x

Gamboa, G., Halfar, J., Hetzinger, S., Adey, W., Zack, T., Kunz, B., & Jacob, D.E. (2010) Mg/Ca ratios in coralline algae record northwest Atlantic temperature variations and North Atlantic Oscillation relationships. *J Geophys Res*, 115. doi: 10.1029/2010JC006262

Halfar, J., Adey, W. H., Kronz, A., Hetzinger, S., Edinger, E., & Fitzhugh, W. W. (2013) Arctic sea-ice decline archived by multicentury annual-resolution record from crustose coralline algal proxy. *P Natl A Sci USA*, 110(49), 19737–19741. doi: 10.1073/pnas.1313775110

Halfar, J., Zack, T., Kronz, A., & Zachos, J.C. (2000) Geochemical signals of rhodoliths (coralline red algae): A new biogenic archive. *J Geophys Res*, 105(C9), 22107–22116. doi: 10.1029/1999JC000128

Halfar, J., Steneck, R., Schöne, B., Moore, G.W.K., Joachimski, M., Kronz, A., Fietzke, J., & Estes, J. (2007) Coralline alga reveals first marine record of Subarctic North Pacific climate change. *Geophys Res Lett*, 34, L07702. doi: 10.1029/2006GL028811

Halfar, J., Steneck, R.S., Joachimski, M., Kronz, A., & Wanamaker, A.D. Jr. (2008) Coralline red algae as high-resolution climate recorders. *Geology*, 36(6), 463-466, doi: 10.1130/G24635A.1.

Halfar, J., Hetzinger, S., Adey, W., Zack, T., Gamboa, G., Kunz, B., Williams, B., & Jacob, D.E. (2011) Coralline algal growth-increment widths archive North Atlantic climate variability. *Palaeogeogr Palaeocl*, 302(1-2), 71-80. doi: 10.1016/j.palaeo.2010.04.009

Halfar, J., Adey, W.H., Kronz, A., Hetzinger, S., Edinger, E., & Fitzhugh, W.W. (2013) Arctic sea-ice decline archived by multicentury annual-resolution record from crustose coralline algal proxy. *P Natl A Sci USA*, 110(49), 19737-19741. doi: 10.1073/pnas.1313775110

Hetzinger, S., Halfar, J., Kronz, A., Simon, K., Adey, W.H., & Steneck, R.S. (2018) Reproducibility of *Clathromorphum compactum* coralline algal Mg/Ca ratios and comparison to high-resolution sea surface temperature data. *Geochim Cosmochim Ac*, 220, 96-109. doi: 10.1016/j.gca.2017.09.044

Hetzinger, S., Halfar, J., Zajacz, Z., & Wisshak, W. (2019) Early start of 20th-century Arctic Sea-ice decline recorded in Svalbard coralline algae. *Geology*, 47, 963-967. doi: 10.1130/G46507.1

Jahn, A. & Laiho, R. (2020) Forced changes in the Arctic freshwater budget emerge in the early 21st century. *Geophys Res Lett*, 47(15). doi: 10.1029/2020GL088854

Kamenos, N.A., Cusack, M., & Moore, P.G. (2008) Red coralline algae are global paleothermometers with bi-weekly resolution. *Geochim Cosmochim Ac*, 72(3), 771–779. doi: 10.1016/j.gca.2007.11.019

Kamenos, N.A. & Law, A. (2010) Temperature controls on coralline algal skeletal growth. *J Phycol*,46, 331-335. doi: 10.1111/j.1529-8817.2009.00780.x

Kaufman, D.S., Schneider, D.P., McKay, N.P., Ammann, C.M., Bradley, R.S., Briffa, K.R., & Miller, G.H. (2009) Recent warming reversed long-term Arctic cooling. *Science*, 325(5945), 1236-1239. http://doi.org/10.1126/science.1173983

Kinnard, C., Zdanowicz, C.M., Fisher, D.A., Isaksson, E., de Vernal, A., & Thompson, L.G. (2011) Reconstructed changes in Arctic sea ice over the past 1,450 years. *Nature*, 479, 509-512. http://doi.org/10.1038/nature10581

Kuffner, I.B., Andersson, A.J., Jokiel, P.L., Rodgers, K.S. & Mackenzie, F.T. (2008) Decreased abundance of crustose coralline algae due to ocean acidification. *Nat Geosci*, 1(2), 114-117. doi: 10.1038/ngeo100

Lebednik, P. (1976) The Corallinaceae of northwestern North America. *I. Clathromorphum* Emend. Adey, *Syesis,* 9, 59-112.

Leclerc, N., Halfar, J., Hetzinger, S., Chan, P.T., Adey, W., Tsay, A., Brossier, E., & Kronz, A. (2021) Suitability of the coralline alga *Clathromorphum compactum* as an Arctic archive for past sea ice cover. *Paleoceanogr Paleoclimatol*, 37. doi: 10.1029/2021PA004286

Leclerc, N., Halfar, J., Porter, T.J., Black, B.A., Hetzinger, S., Zulian, M., & Tsay, A. (2022) Utility of dendrochronology crossdating methods in the development of Arctic coralline red algae *Clathromorphum compactum* growth increment chronology for sea ice cover reconstruction. *Front Mar Sci*, 9. doi: 10.3389/fmars.2022.923088

Muth, A., Esbaugh, A.J. & Dunton, K.H. (2020) Physiological responses of an Arctic crustose coralline alga (*Leptophytum foecundum*) to variations in salinity. *Front Plant Sci*, 19. doi: 10.3389/fpls.2020.01272

Padilla-Gamiño, J.L., Gaitán-Espitia, J.D., Kelly, M.W. & Hofmann, G.E. (2015) Physiological plasticity and local adaptation to elevated pCO_2 in calcareous algae: an ontogenetic and geographic approach. *Evol Appl*, 9, 1043-1053. doi: 10.1111/eva.12411

R Core Team (2019). R: A language and environment for statistical computing. R Foundation for Statistical Computing, Vienna, Austria. URL https://www.R-project.org/.

Rasher, D.B., Steneck, R.S., Halfar, J., Kroeker, K.J., Ries, J.B., Tinker, M.T., et al. (2020) Keystone predators governs the pathway and pace of climate impacts in a Subarctic marine ecosystem. *Science*, 369, 1351-1354. doi: 10.1126/science.aav7515

Ries, J.B., (2006) Mg fractionation in crustose coralline algae: Geochemical, biological, and sedimentological implications of secular variation in the Mg/Ca ratio of seawater. *Geochim Cosmochim Ac*, 70, 891-900. doi: 10.1016/j.gca.2005.10.025

Ries, J.B., A.L. Cohen, and D.C. McCorkle. (2009) Marine calcifiers exhibit mixed responses to CO_2-induced ocean acidification. *Geology*, 37(12), 1131-1134. doi: 10.1130/G30210A.1

Roberts, R.D., Kühl, M., Nøhr Glud, R. & Rysgaard, S. (2002) Primary production of crustose coralline red algae in a high Arctic fjord. *J Phycol*, 38, 273-283. doi: 10.1046/j.1529-8817-2002.01104.x

Rodrigues, J. (2009) The increase in the length of the ice-free season in the Arctic. *Cold Reg Sci Technol*, 59, 78-101. http://doi.org/10.1016/j.coldregions.2009.05.006

Sanders, T., Thomsen, J., Müller J.D., Rehder, G., & Melzner, F. (2021) Decoupling salinity and carbonate chemistry: low calcium ion concentration rather than salinity limits calcification in Baltic Sea mussels. *Biogeosciences*, 18, 2573-2590. doi: 10.5194/bg-18-2573-2021

Schielzeth, H. (2010) Simple means to improve the interpretability of regression coefficients. *Methods Ecol Evol*, I, 103-113. doi: 10.1111/j.2041-210X.2010.00012.x

Spielhagen, R.F., Werner, K., Aagaard Sørensen, S., Zamelczyk, K., Kandiano, E., Budeus, G., Husum, K., Marchitto, T.M., & Hald, M. (2011) Enhanced modern heat transfer to the Arctic by warm Atlantic water. *Science,* 331(6016), 450-453. http://doi.org/10.1126/science.1197397

Steller, D.L., Hernández-Ayón, J.M., Riosmena-Rodríguez, R. & Cabello-Pasini, A. (2007) Effect of temperature on photosynthesis, growth, and calcification rates of the free-living coralline alga *Lithophyllum margaritae*. *Cienc Mar*, 33(4), 441-456. doi: 10.77743/cm.v33i4.1255

Steneck, R.S. (1982) A limpet-coralline alga association: adaptations and defenses between a selective herbivore and its prey. *Ecology,* 63(2), 507-522. doi: 10.2307/1938967

Steneck, R.S. (1986) The ecology of coralline algal crusts: convergent patters and adaptative strategies. *Ann Rev Ecol Syst, 17,* 273-303. doi: 10.1146/annurev.es.17.110186.001421

Westfield, I., Gunnell, J., Rasher, D. B., Williams, B., & Ries, J. B. (2022) Cessation of hardground accretion by the cold-water coralline algae *Clathromorphum compactum* and *Clathromorphum nereostratum* predicted within two centuries. *Geochem Geophys Geosyst*, 23, e2021GC009942. https://doi.org/10.1029/2021GC009942

Williams, B., Halfar, J., DeLong, K.L., Hetzinger, S., Steneck, R.S., & Jacob, D.E. (2014) Multi-specimen and multi-site calibration of Aleutian coralline algal Mg/Ca to sea surface temperature. *Geochim Cosmochim Ac*, 139, 190-204. doi: 10.1016/j.gca.2014.04.006

Williams, B., Chan, P.T.W., Westfield, I.T., Rasher, D.B., & Ries, J. (2021a) Ocean acidification reduces skeletal density of hardground-forming high-latitude crustose coralline algae. *Geophys Res Lett*, 48. doi: 10.1029/2020GL091499

Williams, B., Chan, P.T.W., Halfar, J., Hargan, K., & Adey, W. (2021b) Arctic crustose coralline alga resilient to recent environmental change. *Limnol Oceanogr*, 66, S246-S258. doi: 10.1002/lno.11640

Williams, S., Adey, W., Halfar, J., Kronz, A., Gagnon, P., Belanger, D., & Nash, M. (2018) Effects of light and temperature on Mg uptake, growth, and calcification in the proxy climate archive *Clathromorphum compactum*. *Biogeosciences*, 15, 5745-5759. doi: 10.5194/bg-15-5745-2018

Acknowledgements

The authors are grateful to Jochen Halfar, Eric Brossier, Louis Wilmotte and Natasha Leclerc for their assistance with algal specimen sampling from Arctic Bay, Nunavut, which was integral to this experiment. The authors also acknowledge Isaac Westfield for assisting in the setup of the experimental tank array and to John Gunnell for providing thoughtful input on data analysis. The authors thank Alessio Scurci for his support preparing laboratory specimens and Jochen Halfar for providing expertise on algal sample preparation and laboratory resources. This research was funded by NSF Marine Geology and Geophysics award 1459706 and MIT Sea Grant award NA18OAR4170105 to J.R. and NSERC PGS-D (CGSD3 – 545886-2020) to J.G.

Conflict of interest

The authors are unaware of any personal, professional, or financial conflicts of interest.

Data availability statement

The original data presented in this study are included in the article and will be archived with the Biological and Chemical Oceanography Data Management Office. Further inquiries are welcome and should be directed to the corresponding author.

Author contributions

The experiment was designed by J.G. and J.B.R. and executed by J.G. All data were collected and analyzed by J.G. and interpreted by J.G. and J.B.R. Statistical analyses were developed by J.G. with assistance from J.B.R. J.G. created all data visualizations with input from J.B. The manuscript was written by J.G., with all authors editing the manuscript. All authors approve of its submission.

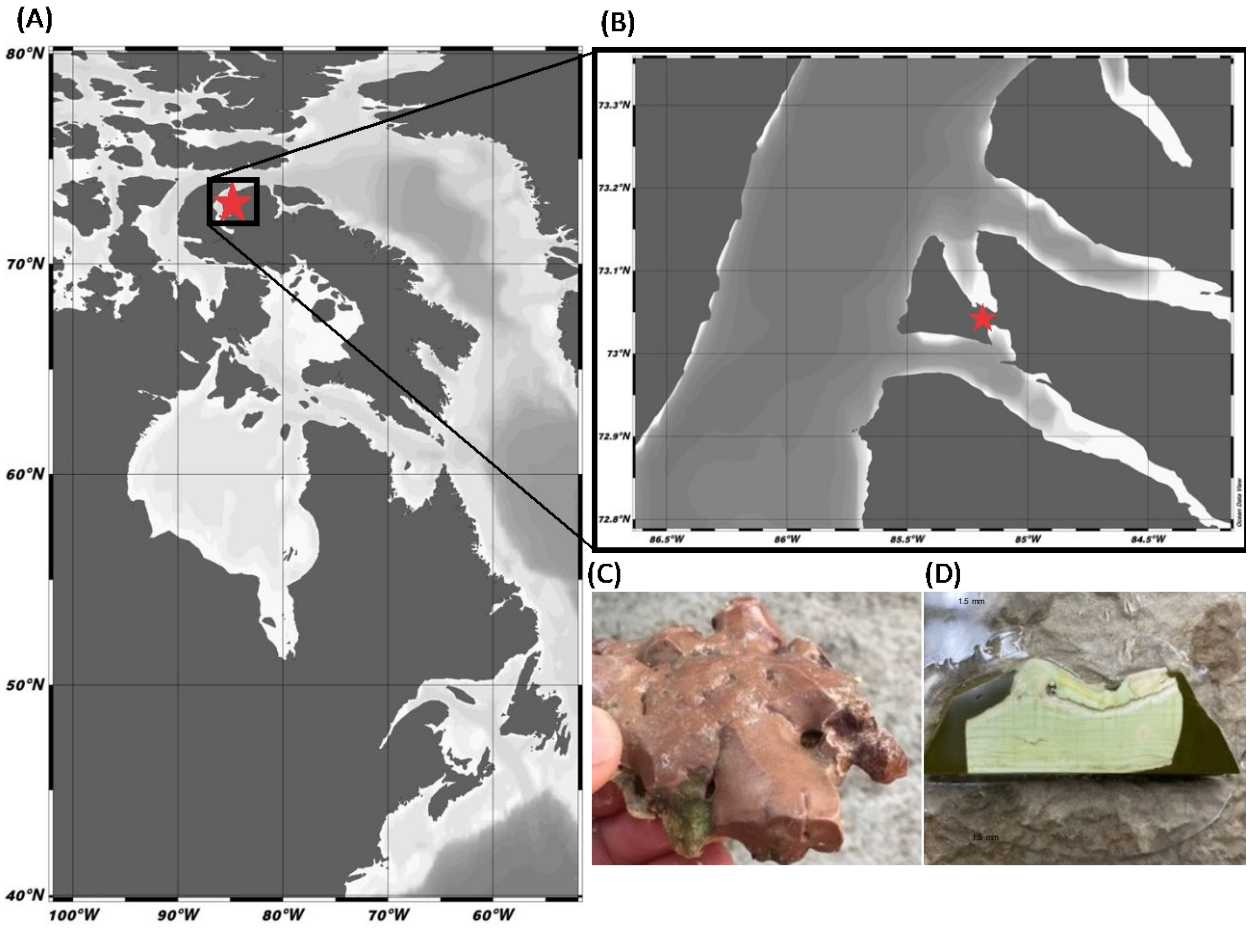

Figure 1. (A,B) Algal sampling location in Arctic Bay, Nunavut, where *Clathromorphum compactum* is commonly found encrusting rocky substrate at ca. 15 meters depth. Representative image of *C. compactum* colony before (C) and after (D) sectioning and polishing for analysis in this study.

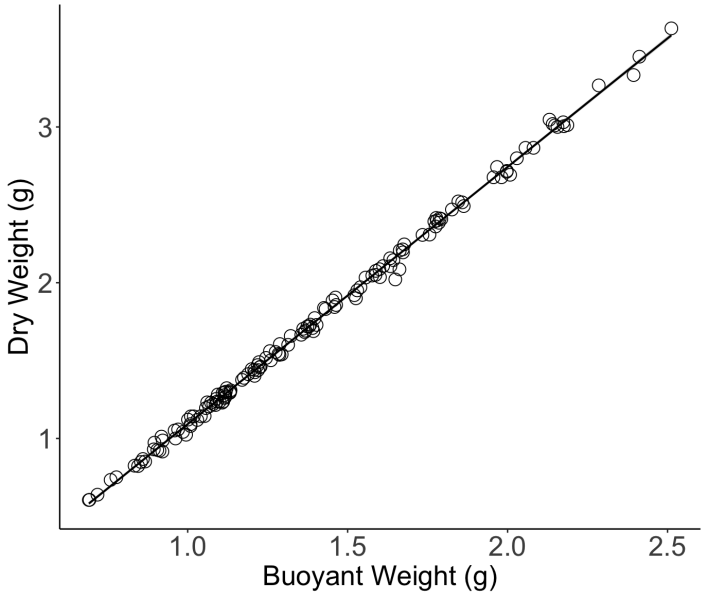

Figure 2. Algal dry-weight to buoyant-weight relationship, Dry Weight (g) = 1.66±0.01(Buoyant Weight (g)) – 0.58±0.01, $p < 2.2x10^{-16}$, SE = 0.05, N = 151, $R^2_{adj} = 0.995$. Points are shaded with a non-opaque grey color to allow visualization of instances where multiple sample points are overlapping.

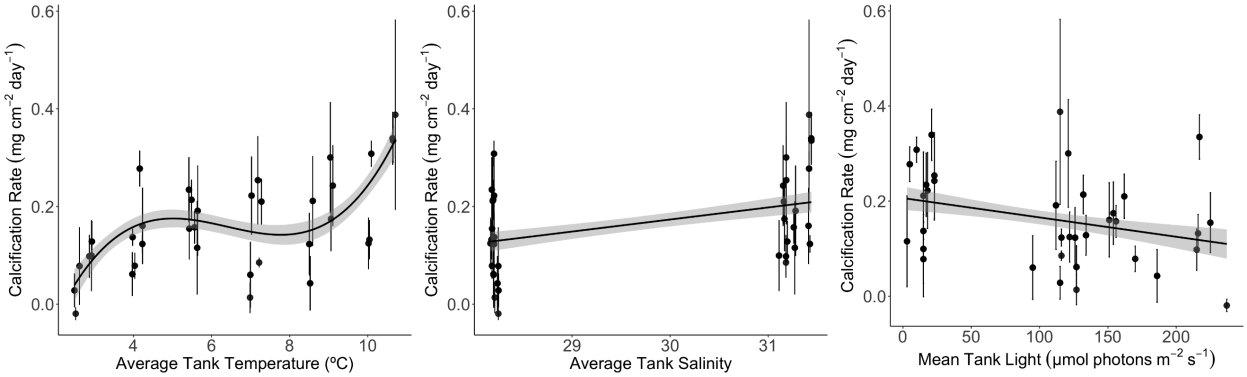

Figure 3. Independent relationships between total algal calcification rate (mg cm^{-2} d^{-1}) and mean tank temperature (T; °C) (calcification rate = $0.38(T) – 0.06(T)^2 + 0.003(T)^3 – 0.56$, p-value < 0.0001, $R^2 = 0.21$), mean tank salinity (S) (calcification rate = 0.024(S) – 0.54, p-value = 0.002, $R^2 = 0.06$), and mean tank light (L; µmol photons m^{-2} s^{-1}) (calcification rate = -0.0004(L) + 0.21, p-value = 0.02, $R^2 = 0.04$). Vertical bars indicate standard error of mean algal calcification rates within a tank (i.e., within a treatment tank). Shading indicates 95% confidence interval of the regressions.

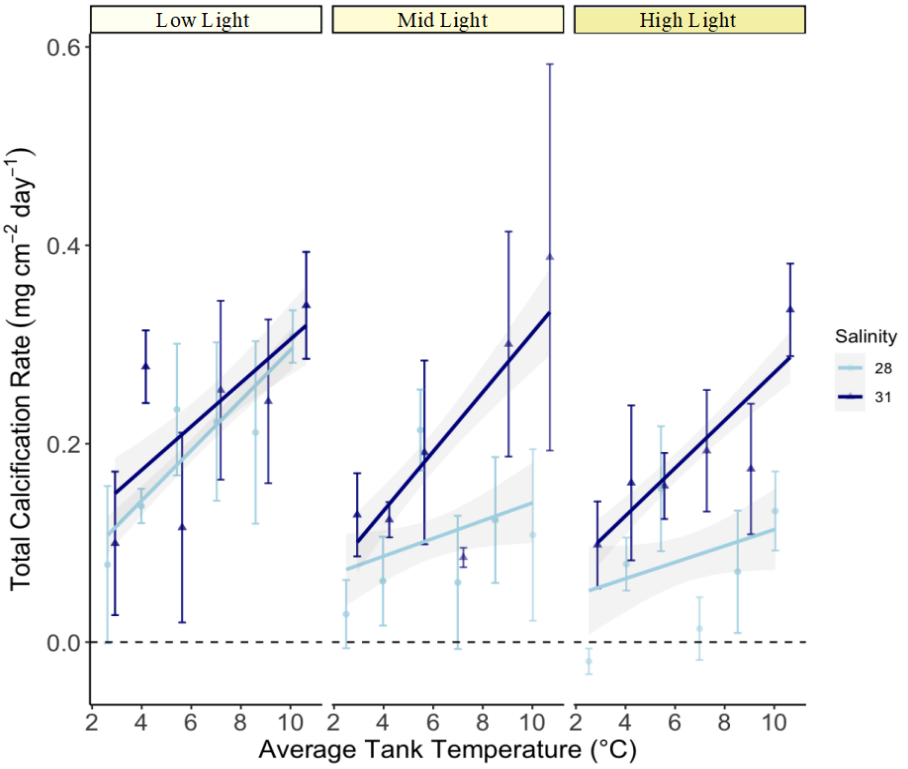

Figure 4. Illustration showing the linear regression relationships between average total algal calcification rate and average tank temperature parsed by salinity and light treatment. Light blue data represent algae growing in low-salinity treatment (salinity treatment target 28), and dark blue data represent algae growing in higher salinity treatment (salinity treatment target 31). Facets separate light treatments showing the relationship across low-, mid-, and high-light treatment tanks. Salinity and light are shown here as categorical variables for illustrative purposes only; all statistical modeling treats them as continuous variables. Each point is indicating the tank average for a given treatment, with vertical bars depicting standard error of tank averages. Light blue and dark blue shading represents 95% confidence interval of the temperature versus calcification rate regressions for the 28 and 31 salinity treatments, respectively.

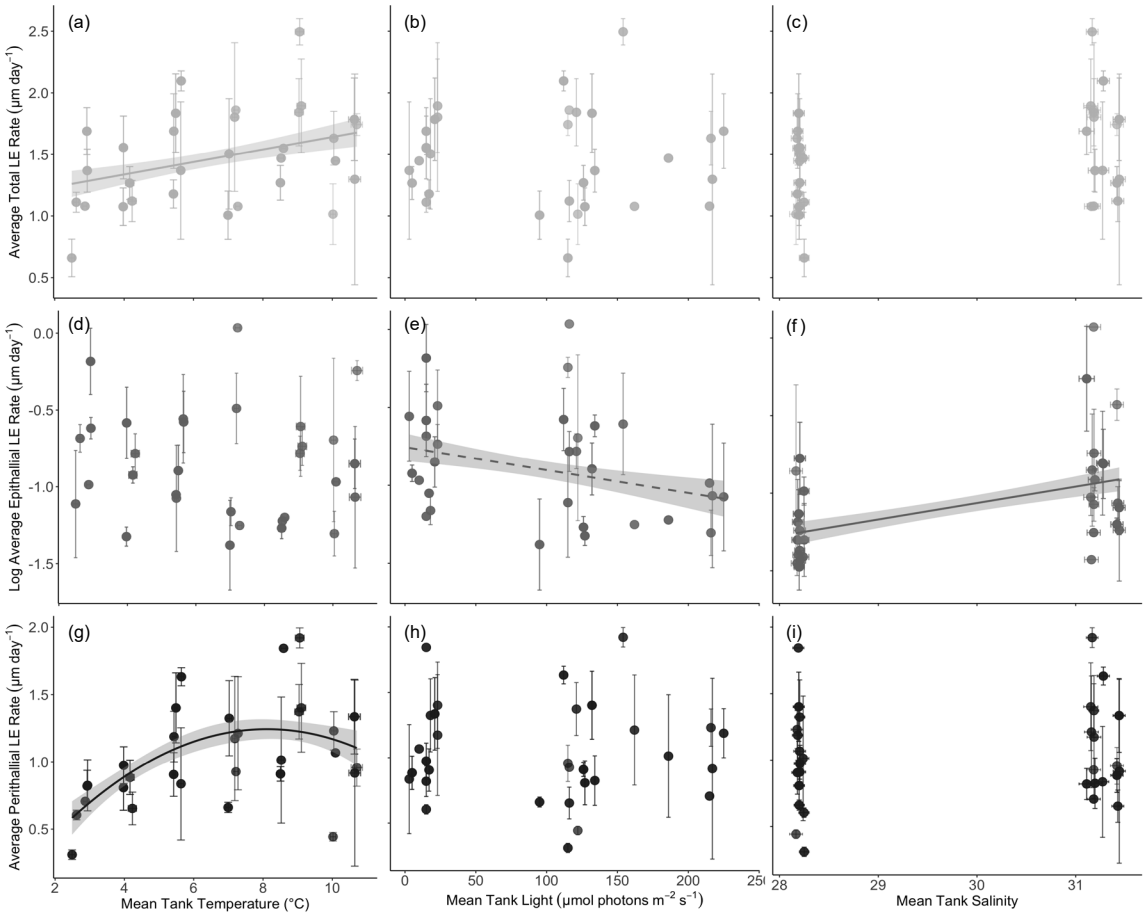

Figure 5. Relationships between average linear extension rates of the total algal skeleton (a-c), the perithallial skeletal layer (d-f), and the epithallial skeletal layer (g-i), and average tank temperature (°C), light (µmol photons $m^{-2}s^{-1}$), and salinity. Vertical bars indicate standard error of tank means, horizontal error bars indicate standard error of tank treatment conditions. Solid (dashed) lines indicate regressions that are statistically significant at the 95% (90%) confidence level (only significant in 4 panels). Shading indicates 95% (a, f, g) and 90% (e) confidence intervals of the regressions.

Table 1. Average ± SE treatment conditions of experimental tanks.

Treatment			T (°C)	Salinity	Light (μmol photons m^{-2} s^{-1})
28 salinity	2.5 °C	Low Light	2.62 ± 0.08	28.25 ± 0.05	15
		Mid Light	2.49 ± 0.08	28.25 ± 0.05	115
		High Light	2.52 ± 0.08	28.25 ± 0.05	237
	4 °C	Low Light	3.98 ± 0.07	28.21 ± 0.06	15
		Mid Light	3.97 ± 0.06	28.20 ± 0.05	127
		High Light	4.03 ± 0.06	28.18 ± 0.05	170
	5.5 °C	Low Light	5.42 ± 0.05	28.18 ± 0.06	17
		Mid Light	5.49 ± 0.05	28.19 ± 0.06	132
		High Light	5.43 ± 0.05	28.18 ± 0.05	225
	7 °C	Low Light	7.02 ± 0.07	28.20 ± 0.05	18
		Mid Light	6.99 ± 0.07	28.20 ± 0.05	95
		High Light	6.99 ± 0.07	28.21 ± 0.05	127
	8.5 °C	Low Light	8.59 ± 0.08	28.19 ± 0.06	15
		Mid Light	8.50 ± 0.08	28.20 ± 0.06	126
		High Light	8.52 ± 0.08	28.24 ± 0.06	186
	10 °C	Low Light	10.09 ± 0.08	28.20 ± 0.06	10
		Mid Light	10.02 ± 0.08	28.17 ± 0.07	122
		High Light	10.04 ± 0.08	28.18 ± 0.06	216
31 salinity	2.5 °C	Low Light	2.93 ± 0.07	31.11 ± 0.08	15
		Mid Light	2.94 ± 0.06	31.20 ± 0.07	134
		High Light	2.87 ± 0.06	31.18 ± 0.07	215
	4 °C	Low Light	4.16 ± 0.12	31.42 ± 0.06	5
		Mid Light	4.23 ± 0.12	31.43 ± 0.06	116
		High Light	4.23 ± 0.12	31.41 ± 0.06	151
	5.5 °C	Low Light	5.63 ± 0.07	31.27 ± 0.06	3
		Mid Light	5.64 ± 0.07	31.28 ± 0.06	112
		High Light	5.56 ± 0.08	31.26 ± 0.06	156
	7 °C	Low Light	7.19 ± 0.07	31.19 ± 0.07	23
		Mid Light	7.22 ± 0.08	31.18 ± 0.07	116
		High Light	7.28 ± 0.07	31.16 ± 0.07	162
	8.5 °C	Low Light	9.10 ± 0.13	31.15 ± 0.07	23
		Mid Light	9.04 ± 0.12	31.18 ± 0.05	121
		High Light	9.06 ± 0.13	31.17 ± 0.06	154
	10 °C	Low Light	10.64 ± 0.17	31.44 ± 0.06	21
		Mid Light	10.71 ± 0.16	31.42 ± 0.07	115
		High Light	10.65 ± 0.17	31.44 ± 0.06	217

Table 2. Average rates of calcification and linear extension data for algal fragments in each treatment. N = 144.

Treatment			Mean Calcification Rate (mg cm^{-2} d^{-1})	SE	N	Mean Total Linear Extension (µm 96 $days^{-1}$)	SE	N	Mean Epithallial Linear Extension (µm 96 $days^{-1}$)	SE	N	Mean Perithallial Linear Extension (µm 96 $days^{-1}$)	SE	N
28 salinity	2.5 °C	Low Light	0.078	0.079	4	86.6	27.87	2	39.6	13.34	2	47.0	14.53	2
		Mid Light	0.028	0.034	4	63.1	14.90	2	33.4	11.38	2	29.7	3.51	2
		High Light	-0.019	0.013	2	NA	NA	NA	NA	NA	NA	NA	NA	NA
	4 °C	Low Light	0.137	0.017	6	105.0	13.67	5	41.0	6.67	5	69.0	5.79	6
		Mid Light	0.061	0.045	6	103.2	14.64	3	25.6	1.54	3	77.6	16.13	3
		High Light	0.079	0.027	3	NA	NA	NA	NA	NA	NA	NA	NA	NA
	5.5 °C	Low Light	0.234	0.067	5	112.9	11.13	4	33.5	0.44	4	86.8	15.70	4
		Mid Light	0.214	0.041	6	135.2	7.52	4	32.3	2.98	5	102.9	8.29	5
		High Light	0.155	0.063	4	137.7	12.78	5	31.5	7.13	4	97.1	4.72	4
	7 °C	Low Light	0.222	0.080	4	144.4	43.06	3	30.3	2.70	3	127.1	26.81	4
		Mid Light	0.060	0.067	5	96.6	18.77	2	25.2	7.15	2	63.5	3.66	2
		High Light	0.014	0.032	2	NA	NA	NA	NA	NA	NA	NA	NA	NA
	8.5 °C	Low Light	0.211	0.092	4	148.8	NA	1	28.9	NA	1	177.0	NA	1
		Mid Light	0.123	0.064	6	121.4	13.10	4	27.1	1.81	4	87.1	4.93	4
		High Light	0.071	0.062	4	139.6	NA	1	28.0	NA	1	96.9	44.94	3
	10 °C	Low Light	0.308	0.026	4	139.0	NA	1	36.5	NA	1	102.5	NA	1
		Mid Light	0.108	0.087	2	72.2	1.59	2	37.9	9.71	2	34.3	11.30	2
		High Light	0.132	0.040	3	156.6	20.96	2	26.3	3.79	2	118.2	13.70	2
31 salinity	2.5 °C	Low Light	0.100	0.072	5	134.6	9.49	3	68.5	11.40	3	66.0	11.20	3
		Mid Light	0.128	0.042	5	131.3	16.78	4	52.1	3.44	4	79.2	18.23	4
		High Light	0.098	0.044	4	103.6	NA	1	35.8	NA	1	67.8	NA	1
	4 °C	Low Light	0.278	0.037	6	121.6	12.78	5	38.3	1.97	5	84.9	12.28	5
		Mid Light	0.123	0.018	4	81.6	11.15	4	34.4	5.00	4	47.1	6.80	4
		High Light	0.160	0.078	4	NA	NA	NA	NA	NA	NA	NA	NA	NA
	5.5 °C	Low Light	0.116	0.096	4	92.9	15.02	2	42.0	0.80	2	55.2	14.99	2
		Mid Light	0.191	0.093	5	158.0	21.95	4	43.9	9.11	4	123.7	19.07	4
		High Light	0.157	0.033	4	NA	NA	NA	NA	NA	NA	NA	NA	NA
	7 °C	Low Light	0.254	0.090	3	125.0	9.82	2	45.0	1.82	2	80.0	11.65	2
		Mid Light	0.085	0.010	2	104.2	NA	1	58.0	NA	1	51.9	NA	1
		High Light	0.193	0.061	3	103.5	NA	1	27.4	NA	1	83.7	7.73	2
	8.5 °C	Low Light	0.243	0.083	3	121.3	6.50	3	32.3	2.32	3	88.4	8.59	3
		Mid Light	0.300	0.113	3	147.5	24.94	3	36.8	2.59	3	110.1	19.29	3
		High Light	0.175	0.066	3	139.7	5.98	2	32.2	10.13	2	107.6	4.16	2
	10 °C	Low Light	0.339	0.054	6	148.2	19.23	5	37.1	2.47	5	111.5	19.80	5
		Mid Light	0.388	0.195	2	97.6	4.95	2	44.0	2.83	2	53.6	7.77	2
		High Light	0.335	0.047	4	81.3	39.28	2	25.6	4.95	2	55.7	34.32	2

Table 3. Summary of most parsimonious final models predicting rates of *C. compactum* linear extension and calcification.

	Parameter	Coefficient ± SE	*t*-value	*p*-value
Total Calcification Rate $R^2 = 0.28$	Intercept	-0.881 ± 0.258	-3.42	**<0.0001**
	Temperature	0.296 ± 0.102	2.892	**<0.01**
	$Temperature^2$	-0.048 ± 0.017	-2.821	**<0.01**
	$Temperature^3$	0.002 ± 0.001	2.889	**<0.01**
	Salinity	0.016 ± 0.007	2.316	**0.02**
	Light	-0.0004 ± 0.0001	-2.608	**0.01**
Total Linear Extension Rate $R^2 = 0.06$	Intercept	1.182 ± 0.154	7.686	**<0.0001**
	Temperature	0.051 ± 0.022	2.269	**0.03**
Log- Epithallial Linear Extension Rate $R^2 = 0.16$	Intercept	-4.092 ± 0.818	-5.000	**<0.0001**
	Salinity	0.109 ± 0.027	3.968	**<0.001**
Perithallial Linear Extension Rate $R^2 = 0.16$	Intercept	-0.162 ± 0.347	-0.467	**0.64**
	Temperature	0.182 ± 0.050	3.116	**0.002**
	$Temperature^2$	-0.152 ± 0.057	-2.667	**0.009**